ARTICLE

Comparison of backbone dynamics of the p50 dimerization domain of NFκB in the homodimeric transcription factor NFκB1 and in its heterodimeric complex with RelA (p65)

Bastian Kohl[1] | Vanessa Granitzka[1] | Amrinder Singh[2] | Pedro Quintas[2] |
Elli Xiromeriti[1] | Fabian Mörtel[1] | Peter E. Wright[2] | Gerard Kroon[2] |
H. Jane Dyson[2] 🄳 | Raphael Stoll[1]

[1]Biomolecular NMR spectroscopy, Ruhr University of Bochum, Bochum, Germany

[2]Department of Integrative Structural and Computational Biology, The Scripps Research Institute, La Jolla, California

Correspondence
H. Jane Dyson, Department of Integrative Structural and Computational Biology, The Scripps Research Institute, Torrey Pines Road, La Jolla, CA 92037.
Email: dyson@scripps.edu

Raphael Stoll, Biomolecular NMR spectroscopy, Ruhr University of Bochum, Universitätsstr. 150, Bochum 44780, Germany.
Email: raphael.stoll@rub.de

Funding information
Deutsche Forschungsgemeinschaft, Grant/Award Numbers: INST 213/757-1 FUGG, INST 213/843-1 FUGG; National Institute of General Medical Sciences, Grant/Award Numbers: GM127807, GM131693, GM71862

Abstract

The nuclear factor of kappa light polypeptide gene enhancer in B-cells (NFκB) transcription factors play a critical role in human immune response. The family includes homodimers and heterodimers of five component proteins, which mediate different transcriptional responses and bind preferentially to different DNA sequences. Crystal structures of DNA complexes show that the dimers of the Rel-homology regions are structurally very similar. Differing DNA sequence preference together with structural similarity suggests that the dimers may differ in their dynamics. In this study, we present the first near-complete ^{15}N, $^{13}C_{\alpha/\beta}$, and H_N backbone resonance assignments of two dimers of the dimerization domain (DD) of the NFκB1 (p50) protein (residues 241–351): the homodimer of two p50 domains and a heterodimer of the p50 DD with the p65 DD. As expected, the two dimers behave very similarly, with chemical shift differences between them largely concentrated in the dimer interface and attributable to specific differences in the amino acid sequences of p50 and p65. A comparison of the picosecond-nanosecond dynamics of the homo- and heterodimers also shows that the environment of p50 is similar, with an overall slightly reduced correlation time for the homodimer compared to the heterodimer, consistent with its slightly smaller molecular weight. These results demonstrate that NMR spectroscopy can be used to explore subtle changes in structure and dynamics that have the potential to give insights into differences in specificity that can be exploited in the design of new therapeutic agents.

KEYWORDS
{^1H} -^{15}N NOE, NFκB1, p50 dimerization domain, protein dynamics, R_1/R_2 relaxation

1 | INTRODUCTION

The nuclear factor of kappa light polypeptide gene enhancer in B-cells (NFκB)[1] is a central transcription factor crucial to

innate/adaptive immunity, cell proliferation, stress response, and apoptosis.[2] The NFκB transcription factor protein family consists of five structurally related subunits that are divided into two classes. Class 1 gene products NFκB1 (p105/p50) and NFκB2 (p100/p52) are synthesized as large precursors

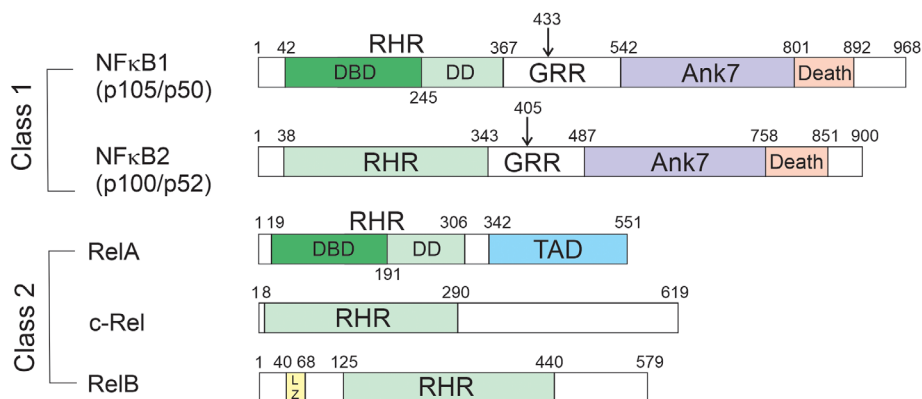Bastian Kohl and Vanessa Granitzka authors contributed equally.

(p105 and p100, which contain ankyrin-repeat domains characteristic of the IκB inhibitors of NFκB) and are processed to give the mature NFκB subunits p50 and p52. Class 2 proteins are also known as Rel proteins.[3] The most common Class 2 protein is RelA (also known as p65), which contains a C-terminal transactivation domain responsible for the recruitment of other transcriptional co-regulators, together with the Rel homology region (RHR) common to all five proteins, which contains DNA-binding and dimerization domains (Figure 1). Homo- or heterodimerization of these proteins creates active NFκB transcription factors. The activity of p50 critically depends on its dimerization status. As a homodimer, p50 acts as a transcriptional repressor for pro-inflammatory genes and as an enhancer for anti-inflammatory genes. [4] The most common heterodimer of p50 is with RelA (p65), which can, for example, activate the expression of interferon-β.[5]

All members of the NFκB protein family contain a conserved RHR, which contains two immunoglobulin-like (Ig) domains. The N-terminal DNA binding domain (DBD) of the RHR mediates specific interaction with the κB consensus DNA sequence 5′-GGGRNNYYCC-3′ (with R as unspecific purine, Y as a pyrimidine and N as any nucleotide), but the entire RHR is required for high affinity binding. The C-terminal dimerization domain (DD) is involved in dimerization, nuclear localization signaling, and interaction with phosphate residues of DNA backbone. In total, NFκB monomers can form 15 different dimers, although many of them have not yet been characterized. The NFκB p50 subunit is derived from its precursor p105 through proteolysis of the ankyrin repeats and the death domain. This cleavage is performed by a co-translational processing event that includes the 26S proteasome.[6] After proteolysis, the p50 RHR consists of ~300 amino acids. Since there is no transactivation domain, the p50 homodimer does not exhibit any transcriptional activity. The 551-amino acid RelA (p65) is the transcriptionally active subunit of the p50/p65 heterodimer and contains the Rel homology domain (~300 residues) and a transactivation domain (TAD). (In the remainder of the paper, we will refer to RelA by its alternative name, p65).

Many structures of DNA complexes of various NFκBs have been solved by X-ray crystallography.[5,7–9] Examples are shown in Figure 2, which shows that the homodimer of p50 (Figure 2a) and the heterodimer of p50 and p65 (Figure 2b) are structurally very similar. Within the κB consensus, the DNA sequences preferred by the homo- and heterodimer differ, and presumably the majority of the difference in DNA affinity and sequence preference is encoded in the DNA-binding domains. Nevertheless, the dimerization domains affect DNA binding, and participate in direct DNA interactions. Unlike the full RHRs, crystal structures have been reported for the dimerization domains alone[10]; the DNA-contacting residues of the dimerization domains remain oriented in these structures similarly to their positions in the DNA-bound full-RHR structures. The present work describes an NMR analysis of a comparison of the solution structural and dynamic behavior of the dimerization domain of p50 in two closely similar environments, designed to determine whether differences in the dynamics of p50 within the two dimers can give insights into differences in DNA sequence preference and other functional differences. The results show that the ps-ns dynamics of homodimeric p50 are extremely similar to those of the same domain in its heterodimeric complex with p65, but that subtle differences are observed between the two dimers that can be directly ascribed to particular amino acids that differ between the partner subunits p50 and p65.

2 | MATERIALS AND METHODS

2.1 | Molecular biology

The gene for p50 DD (residues 241–351 of the mouse sequence, UniProt P25799) was cloned into pET-45b(+) using the restriction enzymes PshAI and HindIII. The sequence included an N-terminal non-native extension (sequence VGTGSNDDDD) derived from the cloning process. The shorter construct used to obtain the ^{15}N relaxation data (residues 248–350 of the mouse sequence) was the same as previously published.[11] The pEt21a plasmid containing the gene for p65 DD (residues 190–321) was the same as previously published.[11]

FIGURE 1 Domain structure in NFκB proteins. Ank7, region containing 7 ankyrin repeats; DBD, DNA-binding domain; DD, dimerization domain; Death, death domain; GRR, glycine-rich region; LZ, leucine zipper domain; RHR, Rel homology domain; TAD, transactivation domain. Numbers indicate sequence positions. The longer proteins of Class 1 are cleaved by proteolysis at sequence positions shown by the vertical arrows
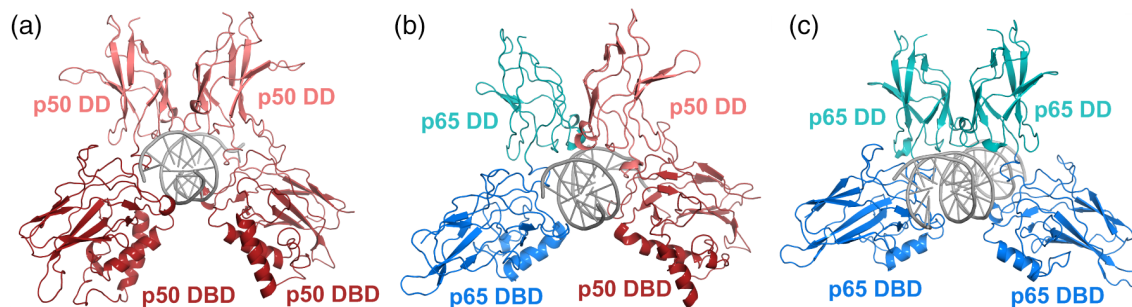
FIGURE 2 Cartoon representation of the X-ray crystal structures of three of the DNA-bound dimers of NFκB. (a) Homodimer of p50 in complex with κB DNA (PDB **1NFK**[7]). DNA sequence TGGGAATTCCC (b) Heterodimer of p50/p65 RHR in complex with κB DNA (PDB **1VKX**[8]). DNA sequence TGGGGACTTTCC (c) Homodimer of p65 with a κB-33 sequence (PDB **2RAM**[26]). DNA sequence CGGCTGGAAATUUCCAGCCG, where U denotes 5-iodo-2′-deoxyuridine-5′-monophosphate. In each structure, gray denotes the DNA, blue the p65 DBD, teal the p65 DD, red the p50 DBD, and salmon the p50 DD

2.2 | Protein expression and purification

For protein expression of p50 DD, the plasmid was transformed into *Escherichia coli*, BL21 T1R applying heat shock transformation. The cells were transferred into LB media supplemented with carbenicillin to grow at 37°C while shaking at 150 rpm for 14 hr. From this LB pre-culture, 1 ml was transferred into HD glucose media supplemented with carbenicillin to grow at 37°C while shaking at 150 rpm for 14 hr. This step was repeated for a second time. The last HD glucose pre-culture was used to inoculate the main culture to an OD_{600} of 0.1. After growing to an OD_{600} of 0.8 the cells were harvested (4,000 g, 10 min, GS-3, Sorvall) and resuspended in $^{13}C/^{15}N/^2H$ isotopically-enriched HD glucose media. After an incubation time of 1 hr, protein expression was induced using 1 mM IPTG at 37°C while shaking at 110 rpm. Expression of triple labelled p50 DD was carried out for 6 hr. Cells were harvested after 8 hr (4,000g, 10 min, GS-3, Sorvall), resuspended in equilibration buffer and stored at −20°C. For protein expression of p65 DD, the plasmid was transformed into *E. coli* BL21 T1R applying heat shock transformation. The cells were transferred into LB media supplemented with carbenicillin to grow at 37°C while shaking at 150 rpm for 14 hr. From this LB pre-culture, 10 ml were transferred into HD acetate media supplemented with carbenicillin to grow at 37°C while shaking at 150 rpm for 14 hr. This step was repeated for a second time. The last HD acetate pre-culture was used to inoculate the main culture to an OD_{600} of 0.1. After growing to an OD_{600} of 0.8 the cells were harvested (4,000g, 10 min, GS-3, Sorvall) and resuspended in ^2H isotopically-enriched HD acetate media. After an incubation time of 1 hr, protein expression was induced using 1 mM IPTG at 37°C while shaking at 110 rpm. Cells were harvested after 8 hr (4,000 g, 10 min, GS-3, Sorvall), resuspended in equilibration buffer and stored at −20°C. The cells were lysed by sonication on ice for 10 min. Cell debris was removed by centrifugation in an SS-34 rotor (Sorvall) at 12,500 rpm at 4°C for 45 min.

All proteins in this study contained a hexa-histidine tag, and were purified using immobilized metal (Ni^{2+}) affinity chromatography (IMAC). First, the column was equilibrated with 2 column volumes (CV) equilibration buffer (Ni NTA). The p50 DD lysate either alone (homodimer) or together with the p65 DD lysate (heterodimer) was loaded onto the column. The unbound molecules were removed using 5 CV equilibration buffer (Ni NTA). Elution was performed by applying a linear gradient ranging from 0% to 100% elution buffer (Ni NTA) and pooled in 3 ml fractions. The flow rate was set to 1 ml/min for every step and observed using UV light at 280 nm. Protein containing fractions were analyzed by SDS-PAGE, pooled together, and concentrated by centrifugation (5,000g, 5810 R, Eppendorf) using a membrane with a molecular weight cut-off (MWCO) of >10 kDa (Amicon). Buffer exchange was carried out with Zeba Spin Desalting Columns (ThermoFisher Scientific) equilibrated with NMR buffer (50 mM HEPES, pH 6.8, 150 mM DTT, 90% H_2O, 10% ^2H_2O). Protein concentration of p50 DD ($\varepsilon = 12,950$ M^{-1} cm^{-1}) homodimer was determined by measuring A_{280} using NanoDrop. For ion exchange chromatography, a Mono Q column was equilibrated with 5 CV equilibration buffer. Then, the p50 DD/p65 DD heterodimer was loaded onto the column and unbound molecules were removed using 5 CV equilibration buffer (Mono Q). The elution was achieved by applying a linear gradient ranging from 0% to 100% elution buffer (Mono Q). Fractions of 200 μl were collected, analyzed by SDS-PAGE, and pooled. Protein concentration ($\varepsilon = 24,410$ M^{-1} cm^{-1}) was determined by measuring A_{280} using NanoDrop. For protein purification of p65 DD a co-purification method was developed since p65 DD His was not expressed in soluble form. The aim of co-purifying p65 DD and p50 DD is getting 1:1 stoichiometry of the heterodimer. However, due to different levels of protein overexpression there was always more p50 DD observed than p65 DD. Therefore, anion exchange chromatography using a Mono Q column was applied to all elution fractions containing p65 DD to obtain a higher concentration of heterodimer. Finally, all

fractions containing 1:1 ratio p50 DD/p65 DD heterodimer were pooled and concentrated using a 10 kDa cut-off membrane, followed by buffer exchange into NMR buffer.

2.3 | NMR spectroscopy

All NMR experiments were carried out on Bruker DRX 600, Avance III HD 700, and Avance III 800 spectrometers. For backbone assignments of the homodimer of the dimerization domain of NFκB1 (p50), a 1.5 mM ^{2}H(70%)/^{15}N/^{13}C-isotopically enriched sample in NMR-buffer was used. For the assignment of H_N, C_α/C_β, and N resonances, TROSY-based deuterium-decoupled versions of 3D HNCACB and HN(CO)CACB spectra were recorded at 298 K on a Bruker Avance III 800 spectrometer. To increase spectral resolution, non-uniform sampling was carried in the ^{13}C dimension. 30% of complex points were recorded and reconstructed by NMRpipe[12] and MDD.[13] Spectra were analyzed using CCPNMR2.7.[14] R_1 and R_2 relaxation data were measured on a 1 mM ^{15}N-labeled NMR sample of the short version (residues 250–352) of the homodimer of the dimerization domain of NFκB1 (p50). Standard Bruker pulse programs[15] were used and data were recorded on a Bruker Avance III HD 700 MHz spectrometer at 298 K. For R_2 relaxation measurements, delays of 0, 10, 30, 50, 70, 90, 110, 130, 150, 170, 190 ms were used. Delays of 20, 100, 140, 180, 200, 300, 500, 750, 1,000, 1,400 ms were used for R_1 relaxation measurements. Relaxation data were processed using TopSpin 3.5 and spectra were analyzed and the data were fitted using CCPNMR 2.7.[14] The correlation time τ_C was calculated by applying the following Equation (1):

$$\tau_c \approx \frac{1}{4\pi\nu_N} \sqrt{6\frac{R_2}{R_1} - 7} \quad (1)$$

Heteronuclear steady-state {^{1}H}-^{15}N NOE spectra[16] were acquired in triplicate with and without presaturation and an interscan delay of 10 s. Resonances were integrated and normalized using the analysis module of the CCPNMR software suite.[14] ^{15}N amide R_1 and R_2 relaxation times were calculated from least squares fitting to a mono-exponential function.

Model-Free analysis of ^{15}N R_1, ^{15}N R_2, and {^{1}H}-^{15}N NOE data sets acquired at 700 MHz for p50 DD homodimer and heterodimer was performed using in-house software[17] incorporating the extended Lipari−Szabo formalism.[18–20] An axially symmetric diffusion tensor was optimized for the p50 DD homodimer [Protein Data Bank (PDB) entry 1NFK], and the p50-p65 DD heterodimer (PDB entry 1VKX) for residues with {^{1}H}-^{15}N NOEs of >0.65 at 700 MHz. The N—H bond length used in the analysis was 1.02 Å and the ^{15}N chemical shift anisotropy was set at −160 ppm. To determine the best model for each residue Bayesian Information Criterion (BIC)[5] was performed after excluding unrealistic models for which $S^2 > 1$, $\tau_e < 0$ ns, and/or $R_{ex} < 0$. Errors in the Model-Free parameters were determined from 500 Monte Carlo simulations.

3 | RESULTS

3.1 | p50 DD backbone resonance assignments

The ^{1}H-^{15}N HSQC spectrum of the homodimeric dimerization domain of NFκB1 (p50 DD) is well dispersed and over 90% of backbone resonances have been assigned (Figure S1). Missing resonances include the backbone amides of Y316, K317, D318, L331, and R332. Resonance assignments for the homodimer of the dimerization domain of NFκB1 (p50 DD) have been deposited at the BioMagResBank under accession number 27915. Secondary structure elements for the p50 dimerization domain in the homodimer, identified from chemical shifts,[21] are consistent with the 10 β-strands (and no α-helices) observed in the crystal structures.
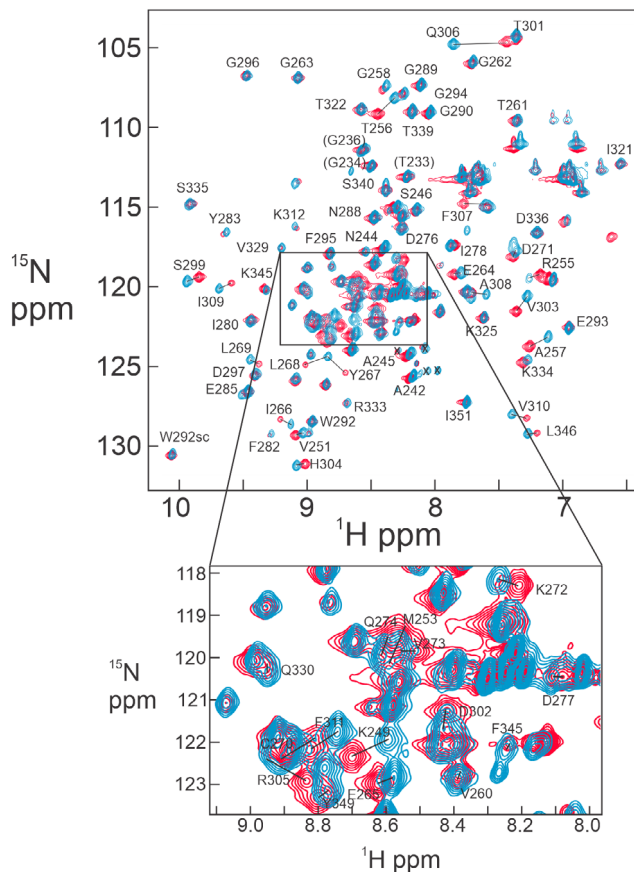

FIGURE 3 Superposition of 2D ^{1}H-^{15}N HSQC spectra of triple labelled p50 DD homodimer (red) and p50 DD in complex with unlabeled p65 DD (blue). The expanded region shows the crowded central region in more detail. Labels in parentheses refer to assignments for a short non-native N-terminal segment
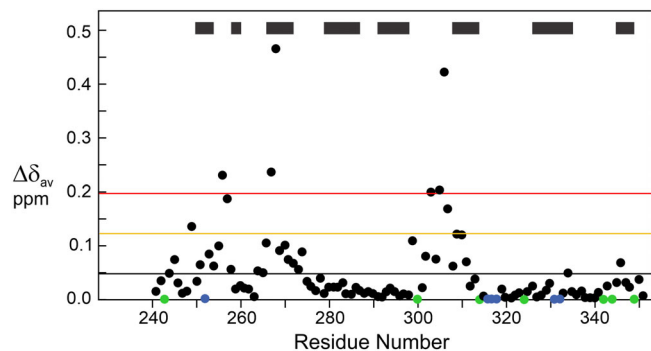
FIGURE 4 Weighted average chemical shift difference $\Delta\delta_{av}$ between p50 DD as homodimer and in complex with p65 DD derived from 2D ^{1}H-^{15}N HSQC spectra. Gray line shows the average chemical shift difference, orange line (average + 1 *SD*) and red line (average + 2*SD*s). Blue dots at the baseline indicate missing dimer-interface resonances in one or both of the spectra. Green dots show the positions of proline residues. The locations of β-strands in the structure of p50 are shown as bars at the top of the figure

The 2D ^{1}H-^{15}N HSQC spectrum of the heterodimer of p50 DD in complex with p65 DD is shown in Figure S2. The missing cross peaks are similar to those seen for the homodimer: residues 316–318 and 331–332, and additionally, R252. Resonance assignments for p50 DD in the heterodimer with p65 DD have been deposited at the Bio-MagResBank under accession number 27916.

The two spectra in Figures S1 and S2 are shown superimposed in Figure 3. Many of the cross peaks are in identical positions; those that differ between them presumably indicate sites of contact on the p50 DD and perhaps slight differences in structure between the two dimers.

The weighted average chemical shift difference $(\Delta\delta_{av} = \sqrt{[(\Delta\delta_H)^2 + (\Delta\delta_N/5)^2]})$ for each assigned residue in the p50 DD sequence is plotted in Figure 4.

3.2 | NMR relaxation experiments

Measurement of relaxation at a residue level can give information on the local motions of the polypeptide chain, and a residue-specific estimate of the flexibility of each part of the protein. For estimates of picosecond-nanosecond motion, three sets of NMR spectra are commonly acquired using protein labeled with ^{15}N: the ^{15}N R_1 (the longitudinal relaxation rate), ^{15}N R_2 (the transverse relaxation rate), and the heteronuclear steady-state {^{1}H}-^{15}N nuclear overhauser enhancement (NOE). The relatively long (non-native) disordered N-terminus of the p50 DD construct complicates the acquisition and analysis of relaxation data.[22] ^{15}N R_1, ^{15}N R_2, and {^{1}H}-^{15}N NOE spectra were therefore recorded for a shorter version of the p50 DD in the homodimer and heterodimer at 298 K and at a proton Larmor frequency of 700 MHz. Relaxation rates were determined by best-fitting of the decay

curve to single exponential function A•e^{-Bx}. Relaxation data have been deposited in the BMRB under accession numbers 27,915 and 27,916. A comparison of the results for the two dimers at 700 MHz is shown in Figure 5. Steady-state heteronuclear {^{1}H}-^{15}N NOEs for well-structured protein regions are usually above 0.8. For p50 DD in both the homodimer and heterodimer, the loop region from residues 287–294 of the sequence that connects two β sheets (Figure 5c) appears to have significantly lower heteronuclear NOE values. The same region shows an upward excursion in R_1 and a downward excursion in R_2.
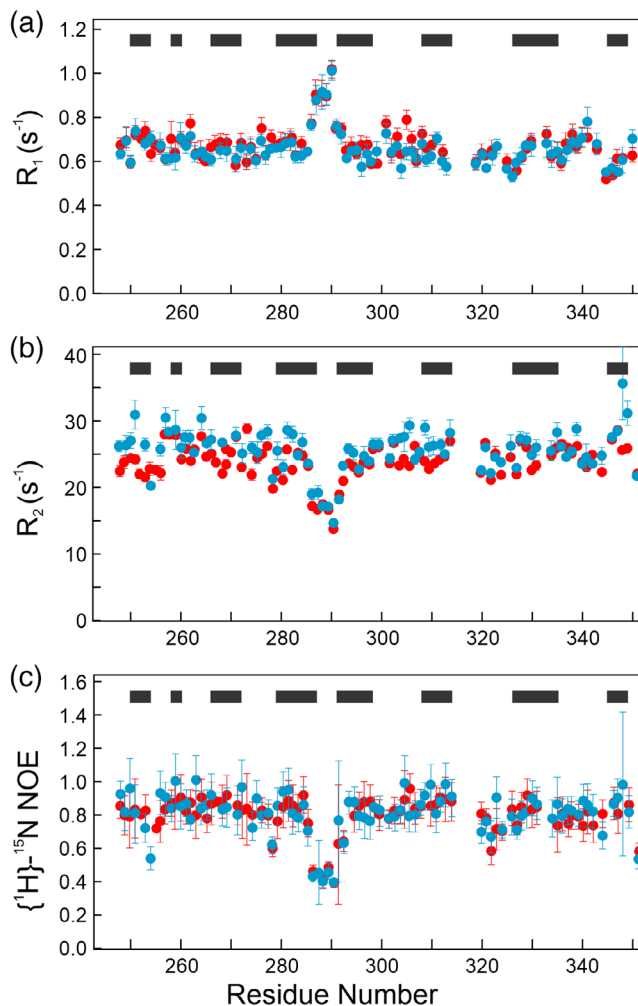

FIGURE 5 Backbone R_1 and R_2 relaxation rates and heteronuclear steady-state {^{1}H}-^{15}N NOE data of p50 DD (250–352) in the homodimer (red) and in the heterodimer (blue), measured at 700 MHz. (a) R_1 relaxation rates. Error bars represent standard deviations from data fitting. (b) R_2 relaxation rates. Error bars represent standard deviations from data fitting. (c) Heteronuclear steady-state {^{1}H}-^{15}N NOE data were recorded in triplicate and averaged. Error bars indicate one standard deviation from the mean of 3 repeated experiments. The locations of β-strands in the structure of p50 are shown as bars at the top of each panel
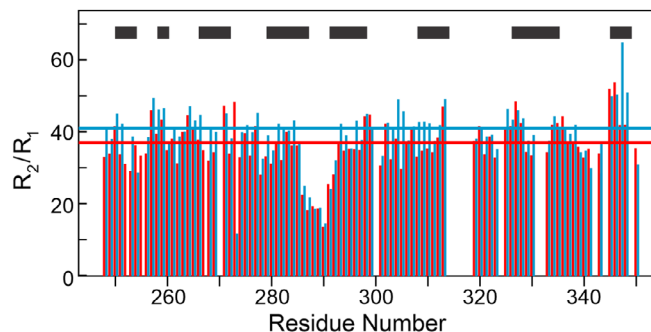
FIGURE 6 R_2/R_1 ratios at 700 MHz for p50 DD (250–352) either as homodimer (red) or in complex with p65 DD (blue). The horizontal red line indicates the average R_2/R_1 value of 36.5 for the structured region of the homodimer, whereas the horizontal blue line marks the average of 39.5 for the same region of the p50/p65 DD heterodimer. The locations of β-strands in the structure of p50 are shown as bars at the top of the figure

The p50 heteronuclear NOE (Figure 5c) and R_1 (Figure 5a) do not show a consistent difference between the homodimer and heterodimer, but there does appear to be a trend in R_2 (Figure 5b) toward lower values for the homodimer. A plot of R_2/R_1 ratio according to the amino acid sequence of p50 DD is shown in Figure 6.

The average R_2/R_1 for the structured core of the p50 DD are 36.5 for the homodimer (red line) and 39.5 for the heterodimer (blue line). The overall trend of the R_2/R_1 ratio is very similar for the two dimers, but the average for the p50 DD homodimer is about 8% lower than for the p50/p65 DD heterodimer. Values for the correlation time τ_c were calculated according to Equation (1) with ν_N as the ^{15}N resonance frequency (see Section 2).[23] This yields τ_c values of 16.6 ns for the 29.5 kDa p50 DD homodimer and 17.3 ns for the 30.1 kDa p50/p65 DD heterodimer.

When the relaxation measurements are obtained for systems that can be described by a single correlation time, they can be further analyzed to give overall estimates of the extent and timescale of local molecular motion using the Model-Free formalism,[18,19] together with the Modelfree computer program.[24] The results of Modelfree analysis for p50 DD in the two dimers are shown in Figure 7. The excursion in the order parameter S^2 for residues 285–290 reflects the data in all three panels of Figure 5, and represents a region that is highly flexible on the ps-ns time scale. In addition, this region shows a consistent contribution of the internal correlation time τ_e for both of the dimers, an indication that this loop is also flexible on a ns time scale. No requirement of an R_{ex} correction is observed for this region, indicating that it is not flexible on the ms time scale. The R_{ex} data shown in Figure 7(c) are widely variable for both dimers, and the presence of so many of them, together with the large number of S^2 values very close to
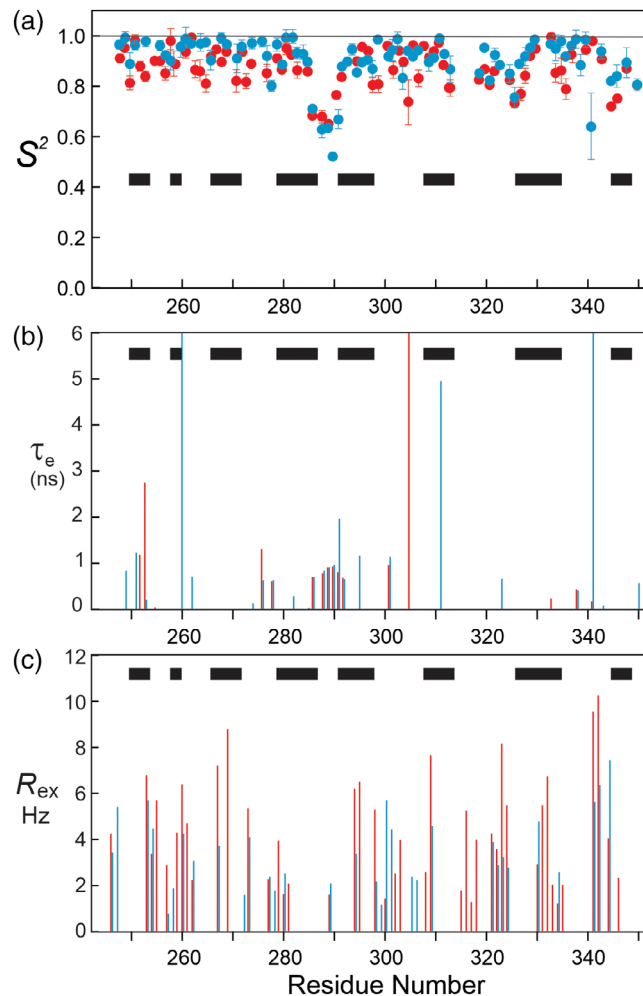

FIGURE 7 Model-free parameters calculated for the homodimer (red) and the heterodimer (blue). β-strands are indicated by black bars in each panel

1, likely indicates that the precision of the relaxation data is not ideal.

4 | DISCUSSION

4.1 | p50 DD is a symmetric homodimer

The resonance linewidths shown for the two spectra in Figure 3 are comparable, indicating that the p50 DD is present as a dimer in both species. A homodimer of p50 is to be expected, as the dissociation constant of the p50 homodimer (0.4 ± 0.05 μM; E. Komives, personal communication) dictates that the molecule would be largely dimeric at the 1.5 mM concentration used for the NMR experiments. The presence of a single set of cross peaks in the ^{1}H-^{15}N HSQC spectrum indicates that the homodimer is symmetric (i.e., the two monomer units have the same structure). The presence of the homodimer was also indicated by the correlation time τ_C calculated from the average R_1 and R_2

relaxation rates. The value of τ_C obtained for p50 under the conditions of the NMR experiments corresponds to a molecular mass of ~30 kDa, consistent with the presence of a dimer rather than a monomer.

4.2 | Chemical shift differences of p50 DD in the two dimers

Assignments for the p50 DD in the homodimer are largely complete, except for residues 316–318, and 331, for which cross peaks in ^{1}H-^{15}N spectra are missing. For p50 DD in complex with p65 DD, cross peaks are missing for residues 252, 316–318, and 331–332. The spectra, particularly those of the heterodimer, also show low-intensity cross peaks in the ^{15}N HSQC for a number of other residues, with the consequence that the assignments for these residues are incomplete due to low signal intensity in the 3D experiments. The low-intensity cross peaks include several residues (R252, D254, Y267, L269, C270) in the dimerization interface.[8]

Resonance assignments for p50 in the two different dimers can be compared directly to give a measure of the difference in the local environment of a given nucleus in the two complexes. Larger values of the average chemical shift difference $\Delta\delta_{av}$ plotted in Figure 4 indicate greater differences between the two environments. Predictably, the greatest chemical shift differences are observed in the dimerization interface. The low intensity of several of the interface resonances, particularly in the heterodimer, is a sign of dynamics in the interface on a time scale of milliseconds or longer. Broadening of resonances in local regions is usually an indicator of exchange between two or more states on a time scale that is intermediate on the NMR chemical shift time scale. In the case of the p50-p65 heterodimer, this observation suggests the presence of breathing motions in the dimer interface. Intriguingly, the residues with low-intensity resonances have been shown by mutagenesis and measurement of binding constants to mediate dimer affinity.[9]

Residues for which the chemical shifts differ between the two dimers more than 1 or 2 SDs from the mean difference (plotted in Figure 4) are shown mapped onto the structures of the two dimers in Figure 8, which also shows the residues for which cross peaks in the ^{1}H-^{15}N HSQC are missing or of low intensity.

Residues that experience the greatest chemical shift differences are clustered in the dimerization interface. Since the data represent differences between the two dimers, the dark red and salmon spheres in Figure 8 are the same in parts A and B. The green spheres, representing weak or missing amide resonances, differ between the two dimers. It is noticeable that two of the residues that show large chemical shift differences, Thr256 and Ala257, are located outside the dimer interface in both dimers. For the p50-p65 heterodimer,
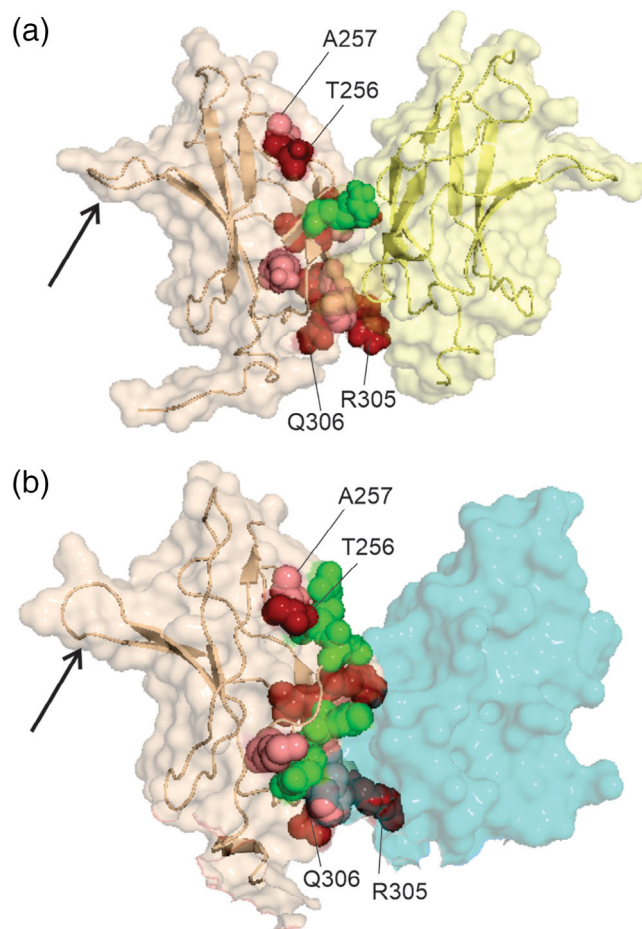

FIGURE 8 Crystal structures of the dimerization domain of p50 in (a) the homodimer (same structure as Figure 2a[7]) and B. the heterodimer with p65 (same structure as Figure 2(b)[8]). Amino acids with (^{1}H, ^{15}N) average chemical shift differences between the homodimer and heterodimer (data from Figure 4) are shown in dark red for differences greater than 2 SDs from the mean and in salmon for differences greater than 1 SD from the mean. The DNA (not shown) is positioned at the bottom of each structure. Residues shown in green have missing or low-intensity cross peaks in the ^{1}H-^{15}N HSQC, likely as a result of exchange between conformers with different structures on an intermediate time scale. The two p50 subunits in the homodimer are shown in pink and yellow in a; only one of the interfaces is highlighted. The p50 subunit is in pink in b, with the p65 subunit in blue. Arrows indicate the flexible loop near residue 290

the green residues, with amide resonances broadened by local exchange processes, are localized between these outliers and the main dimer interface. These results suggest that the outliers experience chemical shift differences between the homodimer and the heterodimer as a result of increased flexibility on a millisecond time scale in the heterodimer. In principle, the relaxation data should give information about this suggestion. If the heterodimer is experiencing exchange in the region 252–255, we would expect to see exchange contributions in the model-free analysis in this region.

Figure 7c shows rather generalized R_{ex} contributions throughout the molecule, and the area around residue 255 shows no difference in R_{ex} between the homo- and heterodimer. As discussed in the following section, the precision of the relaxation data may not be sufficient to make definitive statements on this subject.

The chemical shift changes experienced by individual residues can be ascribed to specific differences in residues in the dimer interface between p50 and p65. For Tyr267, a large perturbation would be expected, since it contacts Phe212 of p65 DD in the heterodimer, one of three interface residues that differ between p50 and p65 monomers. Another residue that discriminates between the homo- and heterodimer interfaces is Asp254. In the heterodimer, there is a hydrogen bond between Asp254 of p50 and Asn199 of p65,[8] which contributes to the stability of the heterodimer.

Interestingly, some of the major chemical shift differences occur close to the DNA-binding interface of the p50DD, located at Arg305 and Gln306 (Figure 8). Structural differences observed between the two crystal structures in this region could be due to differences in the DNA sequences: since different κB DNA sequences are favored by the p50-p50 homodimer and the p50-p65 heterodimer,[8] the crystal structure of p50-p65 heterodimer was solved in complex with 5′-TGGGGACTTTCC-3′ (immunoglobulin κ light-chain gene), whereas the p50 homodimer was crystallized bound to 5′-GGGGATTCCCC-3′.[25] Despite these differences in composition, the orientation of residues in both homo- and heterodimer crystal structures is very similar.[8,25] Bearing in mind that we are studying the free dimerization domains in the absence of either DNA or the attached DNA-binding domains, our observation of large chemical shift differences in this region therefore argues either for a structural change not visible in the crystal, or for a change in local dynamics of the p50 DD in the presence of p65 DD, compared to its homodimer.

4.3 | Backbone relaxation of p50 DD in the homo- and heterodimer

Local picosecond-nanosecond motions of the polypeptide backbone can be estimated using NMR relaxation data. Trends in the relaxation data (Figure 5) are very similar for the p50 DD in the homo- and heterodimer, particularly for the {^{1}H}-^{15}N NOE. Values for residues close to the N- and C-termini are lower than for the majority of the protein, consistent with flexibility at the ends of the protein, as has been observed previously for most other proteins. The {^{1}H}-^{15}N NOE shows a dip around residue 290 in both dimers, corresponding to a flexible loop between two β-strands (indicated by p50DD is present in Figure 8). This loop is the site of the largest temperature factors in the respective crystal

structures.[7,8] The major difference between the homo- and heterodimers is in the R_2 relaxation behavior, which is reflected more clearly in the R_2/R_1 ratio shown in Figure 6. The ratio is consistently lower for the homodimer, giving a smaller overall tumbling time τ_C. The R_2/R_1 ratio is correlated in a general way with the molecular weight: for molecules of the same shape, a larger molecule should have a larger τ_C. The molecular shapes of the two dimers are very similar, and the molecular weights of the homodimer (29.5 kDa) and heterodimer (30.1 kDa) are virtually identical. The difference in the calculated τ_C is small but consistent with the slightly higher molecular weight of the heterodimer.

Calculation of Model-free parameters from the relaxation data obtained for the two dimers showed generally high values of the order parameter S^2, consistent with the all-β structures of the two dimers. Interestingly, the S^2 values recapitulate the small systematic difference in the overall R_2 values shown in Figures 5 and 6. This may be an indication that the precision of the data, collected at only one magnetic field, is lower than would allow us to make definitive statements about differences in this case. The loop region around residue 90 shows increased flexibility, indicated by lowered S^2 values; the flexibility in this region appears to be specifically on a timescale of ~1 ns, as shown by the group of τ_e values around residue 290 (Figure 7b). Both of the dimers show rather generalized exchange contributions R_{ex} throughout the p50 sequence (Figure 7c). This may be an indication that the axially-symmetric model employed in these calculations is not completely appropriate, although other technical issues with data precision and experimental execution may be responsible for the occurrence of generalized exchange contributions and order parameters that anomalously approach 1.

The chemical shift differences between homo- and heterodimers at Arg305 and Gln306 (Figures 4, 8) are not reflected in the ps-ns dynamics shown in Figures 5 and 7. However, Figure 8 shows that these residues are close to a region with low-intensity amide resonances. If these residues are experiencing chemical exchange on an intermediate time scale, we might expect this to be reflected in the R_{ex} terms shown in Figure 7. Again, the precision of the relaxation data does not appear to allow us to observe an enhanced exchange term in this region.

5 | CONCLUSION

The results reported in this work provide an excellent example of the utility of NMR measurements in the characterization of minute differences in structure and dynamics of closely related molecules. Indeed, the entity under study, the p50 dimerization domain, is identical in the two dimers, yet significant differences are seen in their NMR behavior that can be correlated with local sequence differences between

the partner subunits in the homo- and heterodimers. These results provide a basis for further studies of the functionally distinct NFκB dimers, allowing us to address important biological questions, such as the source of differences in DNA sequence specificity, the effects of mutations in the DNA sequence and the molecular-level consequences of drug binding on NFκB-DNA interactions.

ACKNOWLEDGMENTS

ORCID

H. Jane Dyson https://orcid.org/0000-0001-6855-3398

REFERENCES

1. Sen R, Baltimore D. Inducibility of k immunoglobulin enhancer-binding protein NF-kB by a posttranslational mechanism. Cell. 1986;47:921–928.
2. Cartwright T, Perkins ND, Wilson CL. NFKB1: A suppressor of inflammation, ageing and cancer. FEBS J. 2016;283:1812–1822.
3. Nolan GP, Ghosh S, Liou H-C, Tempst P, Baltimore D. DNA binding and IkB inhibition of the cloned p65 subunit of NF-kB, a *rel*-related polypeptide. Cell. 1991;64:961–969.
4. Cao S, Zhang X, Edwards JP, Mosser DM. NF-kappaB1 (p50) homodimers differentially regulate pro- and anti-inflammatory cytokines in macrophages. J Biol Chem. 2006;281:26041–26050.
5. Escalante CR, Shen L, Thanos D, Aggarwal AK. Structure of NF-kappaB p50/p65 heterodimer bound to the PRDII DNA element from the interferon-beta promoter. Structure. 2002;10:383–391.
6. Lin L, DeMartino GN, Greene WC. Cotranslational biogenesis of NF-kappaB p50 by the 26S proteasome. Cell. 1998;92:819–828.
7. Ghosh G, Van Duyne G, Ghosh S, Sigler PB. Structure of NF-kB p50 homodimer bound to a kB site. Nature. 1995;373:303–310.
8. Chen FE, Huang DB, Chen YQ, Ghosh G. Crystal structure of p50/p65 heterodimer of transcription factor NF-kB bound to DNA. Nature. 1998;391:410–413.
9. Sengchanthalangsy LL, Datta S, Huang DB, Anderson E, Braswell EH, Ghosh G. Characterization of the dimer interface of transcription factor NFkappaB p50 homodimer. J Mol Biol. 1999; 289:1029–1040.
10. Huang DB, Huxford T, Chen YQ, Ghosh G. The role of DNA in the mechanism of NFkB dimer formation: Crystal structures of the dimerization domains of the p50 and p65 subunits. Structure. 1997;5:1427–1436.
11. Mukherjee SP, Borin B, Quintas PO, Dyson HJ. NMR characterization of a 72 kDa transcription factor using differential isotopic labeling. Protein Sci. 2016;25:597–604.
12. Delaglio F, Grzesiek S, Vuister GW, Guang Z, Pfeifer J, Bax A. NMRPipe: A multidimensional spectral processing system based on UNIX pipes. J Biomol NMR. 1995;6:277–293.
13. Luan T, Jaravine V, Yee A, Arrowsmith CH, Orekhov VY. Optimization of resolution and sensitivity of 4D NOESY using multi-dimensional decomposition. J Biomol NMR. 2005;33:1–14.
14. Vranken WF, Boucher W, Stevens TJ, et al. The CCPN data model for NMR spectroscopy: Development of a software pipeline. Proteins Struct Funct Genet. 2005;59:687–696.
15. Farrow NA, Muhandiram R, Singer AU, et al. Backbone dynamics of a free and a phosphopeptide-complexed Src homology 2 domain studied by ^{15}N NMR relaxation. Biochemistry. 1994;33:5984–6003.
16. Ferrage F, Piserchio A, Cowburn D, Ghose R. On the measurement of 15N-{1H} nuclear overhauser effects. J Magn Reson. 2008;192:302–313.
17. Bae SH, Legname G, Serban A, Prusiner SB, Wright PE, Dyson HJ. Prion proteins with pathogenic and protective mutations show similar structure and dynamics. Biochemistry. 2009;48:8120–8128.
18. Lipari G, Szabo A. Model-free approach to the interpretation of nuclear magnetic resonance relaxation in macromolecules. 2. Analysis of experimental results. J Am Chem Soc. 1982;104:4559–4570.
19. Lipari G, Szabo A. Model-free approach to the interpretation of nuclear magnetic resonance relaxation in macromolecules. 1. Theory and range of validity. J Am Chem Soc. 1982;104:4546–4559.
20. Clore GM, Szabo A, Bax A, Kay LE, Driscoll PC, Gronenborn AM. Deviations from the simple two-parameter model-free approach to the interpretation of nitrogen-15 nuclear magnetic relaxation of proteins. J Am Chem Soc. 1990;112:4989–4991.
21. Berjanskii MV, Wishart DS. A simple method to predict protein flexibility using secondary chemical shifts. J Am Chem Soc. 2005; 127:14970–14971.
22. Bae SH, Dyson HJ, Wright PE. Prediction of the rotational tumbling time for proteins with disordered segments. J Am Chem Soc. 2009;131:6814–6821.
23. Cavanagh J, Fairbrother WJ, Palmer AG III, Rance M, Skelton NJ. Protein NMR spectroscopy: Principles and practice. Burlington MA: Elsevier Academic Press, 2007.
24. Palmer AG. ModelFree 4.10. (2000).
25. Müller CW, Rey FA, Sodeoka M, Verdine GL, Harrison SC. Structure of the NF-kB p50 homodimer bound to DNA. Nature. 1995;373:311–317.
26. Chen Y-Q, Ghosh S, Ghosh G. A novel DNA recognition mode by the NF-kB p65 homodimer. Nat Struct Biol. 1998;5:67–73.

SUPPORTING INFORMATION

Additional supporting information may be found online in the Supporting Information section at the end of this article.

How to cite this article: Kohl B, Granitzka V, Singh A, et al. Comparison of backbone dynamics of the p50 dimerization domain of NFκB in the homodimeric transcription factor NFκB1 and in its heterodimeric complex with RelA (p65). *Protein Science*. 2019;28:2064–2072. https://doi.org/10.1002/pro.3736